PRIMARY LONGITUDINAL EFFECT IN PLANAR INDUCTION PUMPS DESIGNED FOR HIGH FLOW RATES

L. M. Dronnik, S. Yu. Reutskii, B. N. Siplivyi, and I. M. Tolmach UDC 621.313.53

In boundary-value problems exploring the spatial distributions of the field and currents in induction machines, the resultant field is usually represented as a sum of "external" field which is created in the gap strictly by the currents in the inductor windings and an "internal" field caused by the currents through the liquid metal in the channel.

Due to the discontinuity and the limited length of the inductor, specific effects are observed which are known as the primary longitudinal end effect when dealing with the disbution of the "external" field, and as the secondary end effect, when the subject is the distribution of the "internal" field.

Surveys of work on the longitudinal effect and results achieved are given, in particular in [1-7] and in [8].

In the majority of these investigations the formulation of the problem includes, as far as the inductor is concerned, a so-called shunting zone in the form of an uninsulated magnetic conductor which at both its ends extends beyond the bounds of the actual. This zone may be finite or infinite in length. The wave pattern of the magnetizing current over the insulated portion of the inductor is assumed to be sinusoidal.

In the present treatment in the analysis of the external field configuration we have attempted to rely on a direct experiment designed to measure that field in order to enhance confidence in the following analysis of the secondary longitudinal effect. The investigation was limited to the consideration of inductors in modular systems of high flow rate plane pumps. In such systems the substantial total flow (reaching 20,000 m^3/h) is achieved by parallel connection of several pump modules having lower flow rates (e.g., [9]).

Among others, the following characteristics are found in similar pumps: a sufficiently large number of poles (8-16), the presence of an active converging tube in the first two pole sections, which ensure cavity-free operation at low suction pressures (this provision causes additional field nonuniformity), the desirability to dispense with external cooling of the active inductor materials (by water or nitrogen), which requires the use of heat-resistant electrically insulating materials. It is found that in fulfilling the last requirement the coldest pump location is in the liquid metal inside the operational channel, where the temperature ranges between 300 and 380°C, while the Joule heat produced by the inductor must be disposed of in the liquid metal through the hotter active materials. To minimize overheating, it is necessary to provide a good thermal contact between the windings and the liquid metal channel. This, in turn, establishes the condition for adoption of a coil scheme, where all active elements lie in the grooves within the magnetic conductor. In this case the end sections are also better protected from accidental impacts during the manufacturing process. The technological effectiveness of the production of the sections, including the end sections, is important.

All these conditions greatly limit the selection of the winding type. They are fully satisfied in the so-called Voldek scheme (Fig. 1). In view of the preceding discussion, this scheme can be considered to be typical of high-temperature pumps designed for high flow rates.

We imagine the winding being supplied with one phase of the direct current in the two-sided inductor enclosing the channel. We suppose that the current amplitude equals that of the nominal phase current. We further suppose that the other two phases are disconnected. We shall designate the spatial distributions in the magnetic field intensity in the gap obtained in this case due to currents of each phase A, B, and C by $f_A(x)$, $f_B(x)$, and $f_C(x)$, respectively, where x is the longitudinal coordinate. It is additionally assumed that these distributions do not depend on the perpendicular coordinate and on the coordinate in the channel width direction, which is later substantiated experimentally. Shown in Fig. 2 are the men-

Translated from Magnitnaya Gidrodinamika, No. 2, pp. 91-97, April-June, 1983. Original article submitted September 29, 1982.

0024-998X/83/1902- 0193$07.50

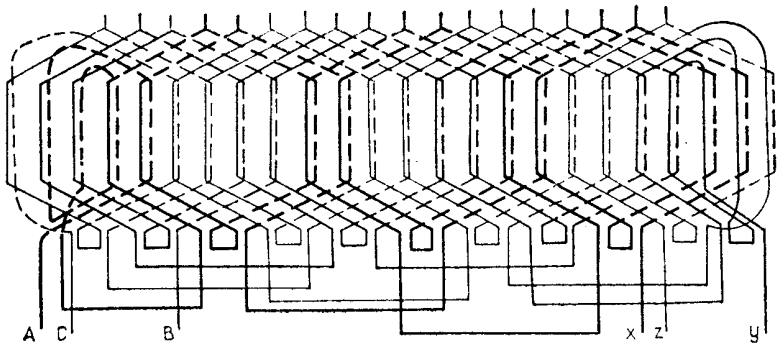

Fig. 1. Voldek's scheme for a three-phase winding of a moving field for an odd number (3) of poles.

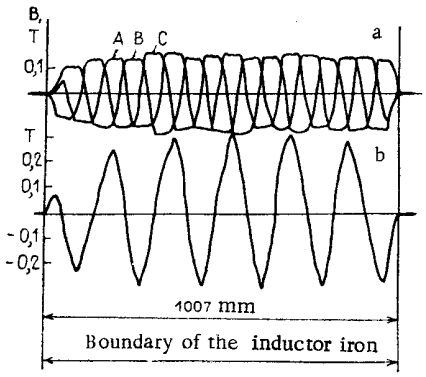

Fig. 2. Experimental results: a) field distribution along the longitudinal coordinate of the multichannel inductor of the the type AMN-6 pump when each phase was supplied with direct current of 139 A while the other two phases were disconnected; b) the resultant external field at the instant t = 0 (for maximum current value in phase A and one-half the amplitude with opposite sign in phases B and C).

tioned distributions measured in an investigation of a small prototype of a pump incorporating modular construction of type AMN-6. This pump, consisting of two modules, produced a design point pressure of 0.43 MPa for a sodium flow rate of 85 liters/sec when the voltage was 360 V and the frequency 148 Hz, resulting in an efficiency for this operating regime of 26% (experimental), which agrees well with the predicted value. The winding scheme in the heat-resistant pump inductors was in accordance with that illustrated in Fig. 1. When operating in the hot regime, when the current was close to the design value, the winding temperature was about 520°C, while that of the sodium was 390°C. The other parameters of the modular pump were as follows: number of poles: 11 (a winding with with an odd number of poles was used), two-layered winding, the width of the active portion of the inductor: 0.194 m, the overall length: 1.007 m, pole pitch: 0.0834 m, number of slots: 72, number of teeth: 73, slot dimensions: 8.9 × 68 mm, tooth dimension: 5 × 68 mm, back edge length: 30 mm. Each slot contained 10 effective conductors, the nominal phase current of an inductor was 98.2 A (effective value). Active converging tubes were provided in the first two pole pitches. The nonmagnetic gap was 18.6 mm and at the entry into the converging tube portion the gap was 28.6 mm.

It is evident from Fig. 2 that the field from the chosen winding type decreases to zero abruptly beyond the longitudinal boundaries of the inductor.

For the same inductor Fig. 3 shows computed field distributions for each phase, as obtained by the method of secondary sources under the following assumptions: absence of slots

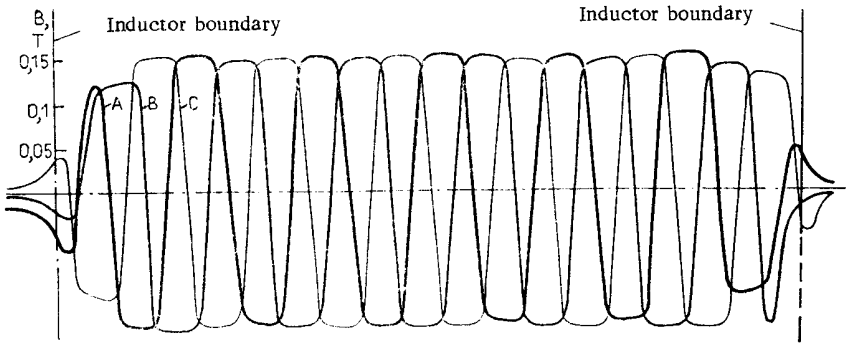

Fig. 3. Computed field distribution in the type AMN-6 for the conditions described in Fig. 2.

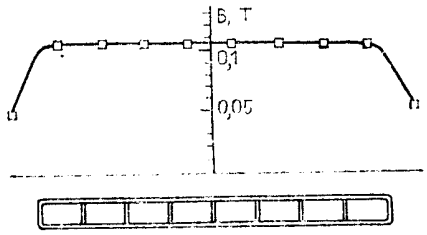

Fig. 4. Field distribution across the channel for phase A current of 100 A and for the longitudinal coordinate value of 0.605 m, measured from the end of converging tube. The experimental points were located at the centers of eight channel sections.

and teeth, the nonmagnetic gap is increased by a ratio determined by the Carter coefficient. On the smooth inductor surface a discrete distribution of currents, corresponding to each slot, is assumed to be in extremely thin layers. These currents equal the total slot current. The field is assumed to be plane-parallel.

A comparison of Figs. 2 and 3 discloses their qualitative agreement. Moreover, the computed field plot provides a transition to the zone beyond the inductor (which is usually found in a plane-parallel arrangement), while the experimental plot indicates a rapid fall-off of the field to zero value outside the inductor zone.

Figure 4 shows the field distribution across the channel for one value of the longitudinal coordinate. It is apparent that within the bounds of the active channel width the distribution is sufficiently uniform.

Taking into account the introduced distributions $f_A(x)$, $f_B(x)$, and $f_C(x)$, the resultant field for a three-phase sinusoidal current supply with a frequency ω will have the form:

$$H(x,t)=f_A(x)\cos\omega t+f_B(x)\cos\left(\omega t-\frac{2\pi}{3}\right)+f_C(x)\cos\left(\omega t+\frac{2\pi}{3}\right). \quad (1)$$

A more general case for nonsinusoidal current has been treated in particular in [10]. However, in a pump with weakly saturated magnetic conductor Eq. (1) applies to sinusoidal external intensity. This has been confirmed by current oscillograms in high-power regimes of the referenced pump AMN-6.

Let expand the distributions $f_A(x)$, $f_B(x)$, and $f_C(x)$ into Fourier series over the length l:

$$f_A(x)=f^0_A+\sum_{n=1}[f^n_{A1}\cos\alpha_n x+f^n_{A2}\sin\alpha_n x];$$

TABLE 1. Four Series Coefficients for the Field Distribution Due to Currents in Each Inductor Phase of the Type AMN-6 Pump. The Reference Phase Current was 139 A

Harmonic	Phase A, mT		Phase B, mT		Phase C, mT	
	f^n_{A1}	f^n_{A2}	f^n_{B1}	f^n_{B2}	f^n_{C1}	f^n_{C2}
0	−0.37	—	2.65	—	0.93	—
1	−13.53	7.38	4.53	2.64	−3.53	−2.76
2	4.68	−4.87	−2.87	7.04	4.48	−13.66
3	13.32	−10.02	−1.14	5.35	4.14	−10.73
4	13.05	−8.13	−4.93	−1.4	3.61	−1.48
5	−2.38	1.78	−1.01	−7.82	−1.63	11.72
6	−20.65	22.44	0.82	−10.63	−15.37	28.54
7	−53.24	41.16	4.32	−23.14	−25.76	47.715
8	104.25	−106.77	8.17	68.52	65.09	−133.25
9	−34.57	47.13	−6.57	−23.37	−20.64	45.09
10	−16.79	18.28	−4.47	−16.14	−9.79	21.26
11	−0.65	−0.5	−1.15	−2.28	−5.62	7.94
12	3.21	−8.49	0.60	2.08	−0.61	−2.93
13	5.12	−5.41	3.59	4.33	3.26	−5.08
14	1.42	−2.44	−0.78	2.38	5.023	−4.77
15	−1.18	4.22	3.32	1.04	2.29	−3.5
16	−2.54	3.32	−2.23	−0.12	−0.33	4.82

$$f_B(x)=f^0_B+\sum_{n=1}\left[f^n_{B1}\cos\alpha_n x+f^n_{B2}\sin\alpha_n x\right];$$
$$f_C(x)=f^0_C+\sum_{n=1}\left[f^n_{C1}\cos\alpha_n x+f^n_{C2}\sin\alpha_n x\right], \tag{2}$$

where
$$n=1,2,3\ldots,\quad \alpha_n=n2\pi/l. \tag{3}$$

The choice of the l value is important in the last parameter. On the one hand, this value must be greater than the inductor overall length by 3-4τ (τ being the pole pitch), i.e., as seen from experiments at each end of the inductor there is an extension zone extending over 1.5-2τ, over which the field has a zero value. This assures practically complete attenuation of currents in the liquid metal over the indicated length in the consequent computation of the secondary effect, since the expansion (2) represents a periodic curve with a period of l (consequently, processes in inductors in adjoining periods will not influence with each other).

On the other hand, l must be so chosen that for some integer value $n = n_k$ the parameter αn_k coincides with $\alpha = \pi/\tau$, corresponding to the fundamental moving wave. In the decomposition shown in Fig. 2, l = 1.33 m (for an inductor length of 1.007 m), while n_k = 8. This condition provides a suffiently rapid elimination of the fundamental moving wave from the general spectrum. Using expansions (2), Eq. (1) for the resultant three-phase field can be identically transformed into the form:

$$H(x,t)=R_{01}\cos\omega t+R_{02}\sin\omega t+\sum_{n=1}\left[L^{\mathrm{I}}_{n1}\cos(\omega t-\alpha_n x)\right.$$
$$\left.+L^{\mathrm{I}}_{n2}\sin(\omega t-\alpha_n x)\right]+\sum_{n=1}\left[L^{\mathrm{II}}_{n1}\cos(\omega t+\alpha_n x)+L^{\mathrm{II}}_{n2}\sin(\omega t+\alpha_n x)\right]. \tag{4}$$

where

$$R_{01}=f^0_A-0.5(f^0_B+f^0_C);\quad R_{02}=\frac{\sqrt{3}}{2}(f^0_B-f^0_C);$$
$$L^{\mathrm{I}}_{n1}=0.5(K^n_1+M^n_2);\quad L^{\mathrm{I}}_{n2}=0.5(M^n_1-K^n_2);$$
$$L^{\mathrm{II}}_{n1}=0.5(K^n_1-M^n_2);\quad L^{\mathrm{II}}_{n2}=0.5(M^n_1+K^n_2),$$

with

$$K^n_1=f^n_{A1}-0.5(f^n_{B1}+f^n_{C1});\quad K^n_2=f^n_{A2}-0.5(f^n_{B2}+f^n_{C2});$$
$$M^n_1=\frac{\sqrt{3}}{2}(f^n_{B1}-f^n_{C1});\quad M^n_2=\frac{\sqrt{3}}{2}(f^n_{B2}-f^n_{C2}). \tag{5}$$

TABLE 2. Amplitudes of the Fluctuating Component of the Forward Running and Reverse Waves in the Inductor of the AMN-6 Pump. Corresponding to an Amplitude of Rated Phase Current of 139 A. a) Fluctuating Amplitude $R_{01}=-2.17$, $R_{02}=1.48$, $\sqrt{R_{01}^2+R_{02}^2}=2.62$; b) Forward and Reverse Running Waves:

Harmonic	Forward, mT			Reverse, mT		
	L^{I}_{n1}	L^{I}_{n2}	$\sqrt{L^{I}_{n1}{}^2+L^{I}_{n2}{}^2}$	L^{II}_{n1}	L^{II}_{n2}	$\sqrt{L^{II}_{n1}{}^2+L^{II}_{n2}{}^2}$
1	−10.08	−1.66	10.21	−9.41	4.13	10.28
2	12.14	−6.68	13.86	−3.58	4.95	6.11
3	15.89	−8.16	17.87	3.01	0.48	3.05
4	11.99	−0.14	12.0	7.58	−2.62	8.02
5	−7.16	7.64	10.48	4.40	−5.22	6.83
6	−35.13	17.97	39.46	2.9	0.75	3.0
7	−69.81	33.01	77.22	−6.17	−1.10	6.27
8	162.66	−101.07	191.50	−9.11	1.52	9.24
9	−55.88	41.05	69.35	1.03	5.452	5.55
10	−25.30	20.79	32.75	1.6	−1.08	1.93
11	−4.99	2.0	5.38	6.76	−1.43	6.91
12	4.58	2.01	5.0	2.57	5.87	6.41
13	5.72	−6.52	8.67	−1.5	−1.28	1.97
14	5.76	−1.85	6.05	−2.72	0.41	2.76
15	0.03	1.21	1.21	−4.98	1.21	5.14
16	−3.78	3.58	5.2	0.69	−1.22	1.4

In Eq. (4) the first two terms on the right-hand side represent the fluctuating field component having a constant spatial amplitude. From a theoretical point of view, it should be equal to zero, since the average values of the functions $f_A(x)$, $f_B(x)$, and $f_C(x)$ over the period l in an induction machine are equal zero.

The next pair of terms under the summation sign represent the spectrum of the forward running wave, moving in the positive direction. The last two terms represent the spectrum of the reverse wave. In Eq. (4) combinations of the type $R_{01}\cos\omega t + R_{02}\sin\omega t$ have not been presented in the form $R_0\cos(\omega t+\varphi_0)$, since the multiple value in the choice of the φ_0 parameter may lead to errors.

Starting with Eq. (4) it is possible to write another equivalent form for the equation which does not contain the backward running wave. This follows from the recognition that each reverse harmonic can be added to a portion of the corresponding forward wave having the same amplitude. In summation this produces the fluctuating component with an amplitude, which depends on the x-coordinate:

$$H(x,t)=\left[R_{01}+\sum_{n=1}2L^{II}_{n1}\cos\alpha_n x\right]\cos\omega t+ \\ +\left[R_{02}+\sum_{n=1}2L^{II}_{n2}\cos\alpha_n x\right]\sin\omega t+\sum_{n=1}[(L^{I}_{n1}-L^{II}_{n1})\cos(\omega t-\alpha_n x)+(L^{I}_{n2}-L^{II}_{n2})\sin(\omega t-\alpha_n x)]. \quad (6)$$

In Eq. (6) the first two terms on the right-hand side constitute the fluctuating component, while the following two give the spectrum of the forward running harmonics.

For the field of the pump AMN-6 the amplitude spectrum (2) was obtained based on 80 terms in the Fourier series. However, only the first 16 harmonics have practical significance; in the remaining "tail" only a few amplitudes reach 2% of the maximum value of a single phase induction, the remainder attaining less than 0.5%.

Listed in Table 1 are the values of Fourier coefficients obtained by computer expansion of the plots shown in Fig. 2 according to Eq. (2). From these values, based on Eqs. (4) and (5), amplitudes of the components have been evaluated and tabulated in Table 2. Using values in that table, amplitude distributions of forward running and reverse waves as functions of the n number are shown in Fig. 5. (Only integer positive values of n have meaning.)

The distribution of the resultant external field at the instant t = 0 was computed from distribution (4) and the harmonic amplitudes listed in Table 1. This computed distribution practically coincided with the experimental distribution shown in Fig. 2b for the same time

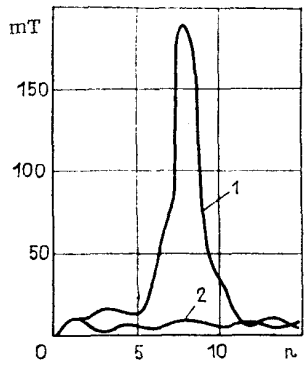

Fig. 5

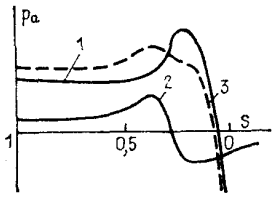

Fig. 6

Fig. 5. Amplitude distribution of forward (1) and reverse running (2) waves as a function of the harmonic number n.

Fig. 6. Qualitative estimate of the influence of the higher harmonics of the external field on the pressure-flow rate characteristic: 1) based on the fundamental harmonic; 2) based on the highest harmonic; 3) combined characteristic.

instant. This indirectly confirms the correctness of the calculation of the Fourier coefficients.

From the tabulated results and the curves plotted in Figs. 2 and 5 the following conclusions can be drawn:

1. In the Voldek winding employed the external field drops to zero practically at once beyond the inductor boundary (in the longitudinal direction), whereas the transverse distribution is essentially uniform across the channel width. Keeping in mind that there is practically no external field beyond the inductor boundaries, it must be assumed that an inherent (induced) field in those segments is also close to zero, which facilitates the solution of the boundary-value problem taking into account the secondary effect. As made apparent in Fig. 2a, the influence of the teeth is not significant.

2. The amplitude of the fluctuating component in expansion (4) $\sqrt{R_{01}^2+R_{02}^2}=2.63$ mT, thus constituting less than 1% of the resultant field amplitude. This result agrees with the preceding discussion where it was argued that this amplitude should, in fact, equal zero. The presence of a small component in the experiments is tied in with errors in the field computation and in the numerical data function.

3. The amplitudes of the reverse waves are relatively small; their greatest surge (for n = 1, 4, 8, 11, and 15) do not exceed 10 mT, i.e., 3% of the amplitude of the resultant field.

4. The forward running wave spectrum contains a peak of the fundamental harmonic with n = 8; this had been anticipated in the selection of l as the expansion period. However, besides the fundamental harmonic, the 9th and 10th harmonics are sufficiently noticeable. They move with a velocity that is below that of the 8th, 7th, 6th, and 3rd harmonics which run forward at a high velocity. It is because of this situation that relative to the fundamental wave, regimes with reverse slip are possible in the harmonics with n > 8, i.e., regimes typical of generators. Taking into account that the velocity of the moving field for the n-th harmonic equals $v_{sn} = \omega/\alpha_n$, generator regimes for harmonics with n > 8 are possible when the following condition is satisfied:

$$\frac{n}{8}(1-s_n)>1, \tag{7}$$

where $s_n = 1 - (v_M/v_{s8})$ is the nominal slip and v_M is the average nominal velocity of the moving liquid metal.

5. As made apparent in Fig. 5, there exist more "intimate" properties in the mutual amplitude distributions of the forward and reverse waves: for instance, in the zones of the minimum amplitudes of the reverse harmonics one finds the maximum amplitudes of the forward harmonics. The fundamental harmonic (n = 8) constitutes an exception, since in this instance both waves have their maxima.

6. The presence of a spectrum of forward running waves (rather than there being a single fundamental) evidently can significantly influence, together with other factors, the p(Q) characteristic, especially if one takes into account the possibility of the formation of generator regimes for the higher harmonics.* This is qualitatively indicated in Fig. 6, where the curve 1 is a plot of the pressure-flow rate pump characteristic in the presence of a single fundamental wave of the moving field, while curve 2 is the same characteristic when only the upper harmonic is acting. By admitting in the qualitative estimate the superposition principle, we obtain the resultant p(Q) characteristic 3, wherein the characteristic maximum of the characteristic 1 is partially suppressed by the generator regions of the characteristic 2. (It is understood that for quantitative evaluations the superposition method is unsuitable.)

The features of the "external" magnetic field distribution for the multipole inductor with the chosen winding muxt be included in the solution of the secondary longitudinal effect problem.

LITERATURE CITED

1. A. I. Voldek, Inductive Magnetohydrodynamic Devices with a Liquid Metal Working Medium [in Russian], Énergiya, Leningrad (1970).
2. G. A. Baranov, V. A. Glukhikh, and I. R. Kirillov, Computation and Design of Inductive MHD Devices with Liquid Metal Working Medium [in Russian], Atomizdat, Moscow (1978).
3. I. R. Parts, Theoretical and Experimental Investigation of Inductive Devices with Open Magnetic Conductors [in Russian], Valous, Tallin (1972).
4. Yu. K. Krumin, Interaction of a Moving Magnetic Field with a Conducting Medium [in Russian], Zinatne, Riga (1969).
5. Ya. Ya. Lielpeter, Liquid Metal MHD Devices [in Russian], Zinatne, Riga (1969).
6. A. Ya. Vilnitis and M. S. Drits, End Effect in Linear Asynchronous Motors [in Russian], Zinatne, Riga (1981).
7. T. K. Kalnin, Linear Inductive Devices with a Transverse Magnetic Flux [in Russian], Zinatne, Riga (1980).
8. A. P. Rashchenkin, "Electrical characteristics of linear inductive MHD devices, taking into account the end effects," Magn. Gidrodin., No. 2, 110-118 (1968).
9. L. M. Dronnik, O. A. Omelchenko, V. E. Strizhak, I. M. Tolmach, E. I. Kirisik, V. G. Smirnov, and Yu. P. Ushakov, "Multichannel inductive electromagnetic pump," Inventor's Certificate No. 748749, Byull. Izobret., No. 26 (1980).
10. D. S. Kovner and V. G. Smirnov, "Analysis of the moving magnetic field and of the volume force field in the channel of a plane induction pump," Magn. Gidrodin., No. 4, 86-92 (1981).

*This circumstance was pointed out by L. Ya. Ulmanis.